Contents

Project overview

1.1 Abstract

Genetically-encoded biosensors have revolutionized our ability to measure a wide variety of cellular properties in live animals. As experimentalists, any time a new sensor is developed, we would like to know: what is that sensor good for? That is, what range of values of the cellular property of interest is that sensor well-suited to measure accurately? Here, we present a theoretical framework to determine the suitability of biosensors with two states.

Two-state biosensors are simple sensors that change conformation, and spectral properties, in response to a specific input. Existing two-state biosensors respond to a wide variety of important cellular properties, including pH, ATP, and glutathione redox potential. In our previous work with the roGFP1_R12 sensor, we deployed a mathematical framework that enabled us to calculate glutathione redox potential from fluorescence ratio measurements given knowledge of the spectral and biochemical properties of the sensor, and the properties of our microscope.

We extended this framework to analyze how the precision of microscopy measurements limits the accuracy of calculated glutathione redox potentials. This enabled us to predict the range of redox potentials that roGFP1_R12 is well-suited to measure given a theoretical measurement error and, importantly, with our empirically-determined measurement error. This analysis demonstrated that our sensor is well-suited to measure cytosolic glutathione redox potential in the feeding muscles of live *C. elegans* over a wide range of environmental and genetic conditions.

Next, we applied our theoretical framework to 10 glutathione redox potential sensors with known spectral and biochemical properties. This enabled us to define the range of potentials for which each sensor is well-suited and choose optimal sensors for different applications. Finally, we generalized our framework to all ratiometric two-state biosensors and applied this analysis to families of pH and nucleotide-specific biosensors. To increase the accessibility of our framework, we have also built web-based, interactive tools and documentation to help the community find biosensors that are well-suited for their experiments.

1.2 Background

Biosensors are usually genetically-encoded proteins that emit fluorescence. A well-known one-state sensor is the wild-type green fluorescent protein (GFP). When GFP is excited by light, it fluoresces and emits light around $510\ nm$. The relative amount of light emitted depends on the wavelength that initially excited the sensor (Figure 1). GFP is used for a wide variety of research purposes, such as visualizing the localization of cellular proteins.

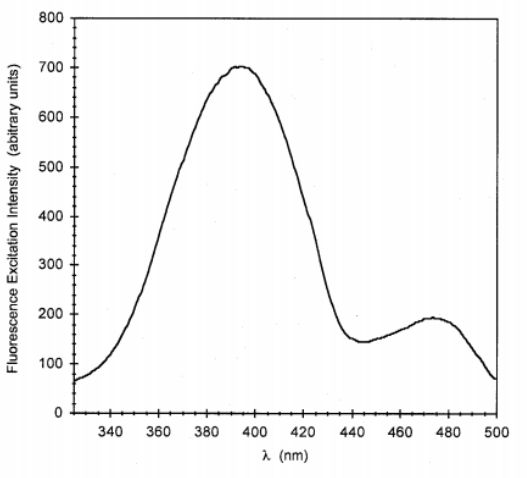

Figure 1. The emission spectra of wild-type GFP when emitted light is captured at 510 nm. Image from Mark Cannon's 2005 Thesis (personal correspondence).

Chemists have modified GFP to be sensitive to properties such as pH and glutathione redox potential. Many of these modified GFPs exist in two states. For example, redox-sensitive GFPs (roGFPs) are proteins that can exist in either an oxidized or a reduced state [1-3]. Since each state has a unique fluorescence emission pattern, knowledge of (1) the concentration of sensors and (2) the level of fluorescence emission at a certain wavelength can be used to determine the proportion of sensors in each state (Figure 2).

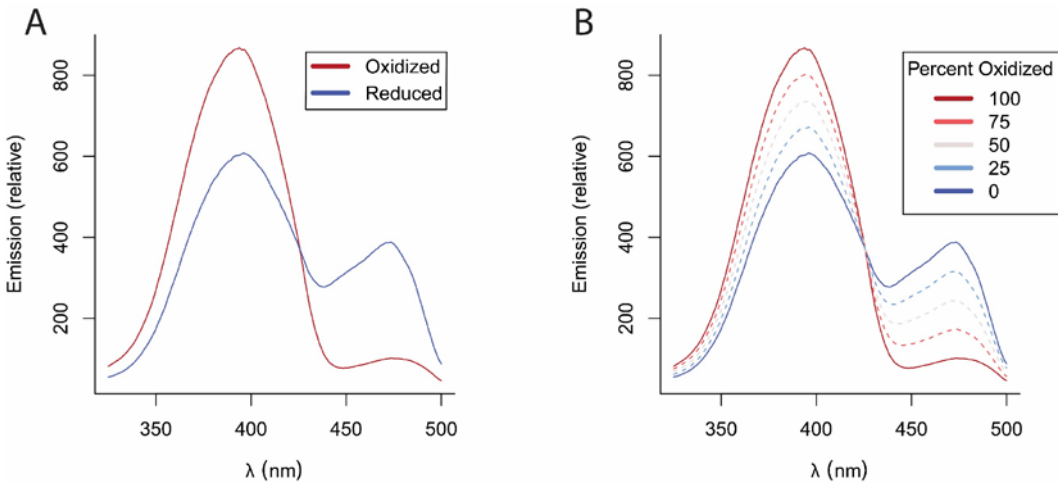

Figure 2. The emission spectra of the redox sensor roGFP1-R12. (A) Emission spectra of oxidized and reduced forms of the sensor. (B) Weighted spectra of a population of sensors along with the corresponding proportion of oxidized sensors.

Figure 2. The emission spectra of the redox sensor roGFP1-R12. **(A)** Emission spectra of oxidized and reduced forms of the sensor. **(B)** Weighted spectra of a population of sensors along with the corresponding proportion of oxidized sensors.

Intensity measurements from simple fluorescent microscopy can be used to determine the fraction of redox sensors that are oxidized, but those measurements also depend on concentration, which is typically unknown. To obtain a concentration-independent indication of the fraction of sensors in each state, we use a ratio image from two different excitation wavelengths. Using the ratio image, we can create a unique map between fluorescence emission and redox potential. We have previously used ratiometric microscopy to make highly precise measurements in *Caenorhabditis elegans*, which have revealed novel insights into the intercellular organization of redox potential [4].

The ratio of sensor emissions taken at the two wavelengths R, is related to the proportion of sensors in an oxidized or reduced state. At the minimum ratio value (R_{min}), all sensors are reduced. As sensor molecules become oxidized, the emission in the $410\ nm$ increases and the emission in $470\ nm$ decreases. When the ratio emission reaches its maximum value (R_{max}), all sensors are oxidized. Previous groups have created functions that map between observed ratiometric measurement (R) and the fraction of oxidized sensor molecules (OxD), which is used as an input to the Nernst equation to determine the cellular redox potential (E) (Figure 3, Supplementary Material 1) [5].

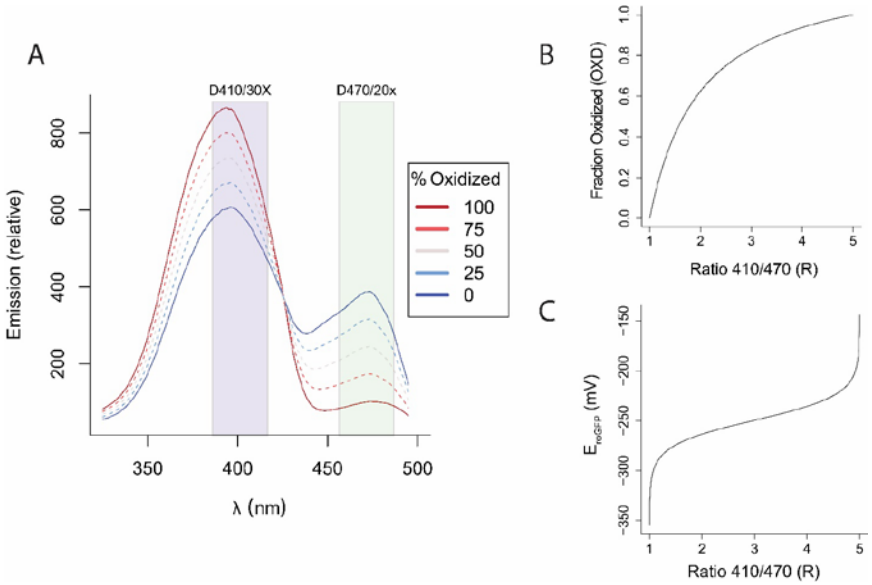

Figure 3. The ratiometric properties of roGFP1-R12 and their maps to redox measurements. (A) The fluorescence emission spectra of roGFP1-R12. Ratiometric measurements can be made by exciting with light passed through filters such as D410/30X and D470/20X, shown as translucent rectangles. As the percentage of oxidized sensors changes, so does the distribution of emission around the isosbestic point. ***(B)*** *The map between ratio measurement and fraction oxidized, described by the equation* $OxD = \frac{R-R_{min}}{(R-R_{min})-\delta_2(R-R_{max})}$ *where* R *is the ratiometric measurement,* R_{min} *is the ratio when fully reduced,* R_{max} *is the ratio when fully oxidized, and* δ_2 *is the relative contribution of the second wavelength (in this case,* $470\ nm$*) to the dynamic range.* ***(C)*** *The map between ratio measurement and redox potential, described by the equation* $E = E^\circ - \frac{R_{gas}T}{2F}\ln(\frac{1-OxD}{OxD})$ *where* E *is the redox potential,* E° *is the midpoint potential,* R_{gas} *is the gas constant,* T *is the temperature in Kelvin, and* F *is the Faraday constant.*

1.3 Results

1.3.1 Microscope precision limits the accuracy of measurements from roGFP1-R12

We modeled how microscopy errors affect glutathione redox potential estimates with the roGFP1-R12 sensor. Empirically, our microscope's error was approximately 3%, with the observed ratio $R_{Observed} = R_{True} * (1 \pm 0.03)$. We observe that our error in R can have disproportionally large effects on redox potential estimates, especially near minimum and maximum limits of the sensor. For example, 3% microscopy errors recorded at $R = 0.69$ and $R = 5.15$ each cause misestimations of over $50\, mV$ (Figure 4).

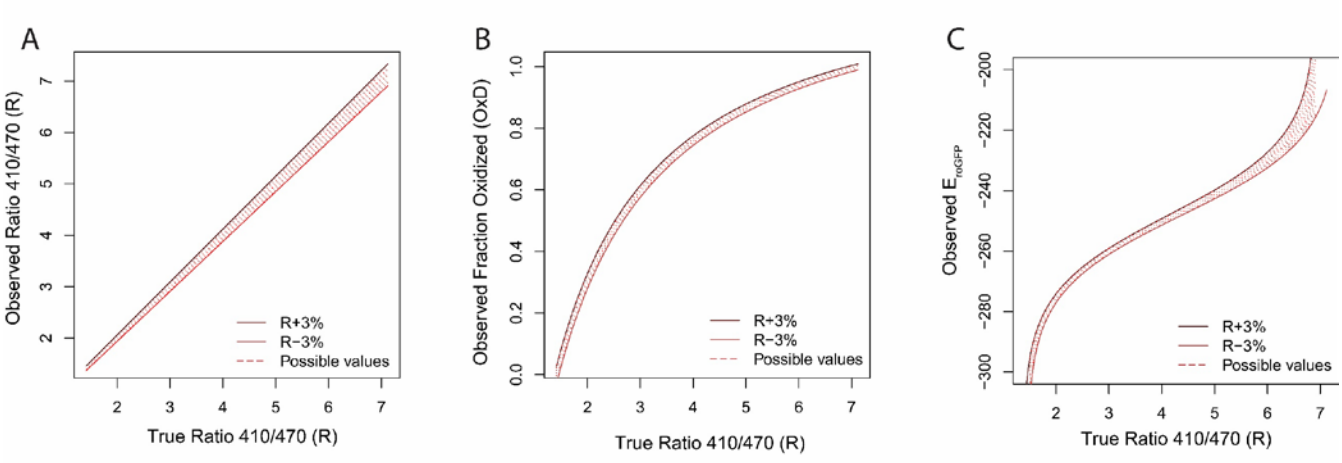

Figure 4. (A) Our empirically-observed error model of $R_{Observed} = R_{True} * (1 \pm 0.03)$. **(B)** The effect of 3% microscopy error on the estimate of fraction oxidized (OxD). **(C)** The effect of 3% microscopy error on the estimate of glutathione redox potential (E_{GSH}).

1.3.2 Our framework estimates the values roGFP1-R12 is well-suited to measure

When the error in ratio measurements propagates to the estimate of the glutathione redox potential, all estimates of redox potential have some associated error. For any true redox potential, there is a range of redox potentials that you could observe.

1.3.3 Our framework applies to other glutathione redox potential sensors

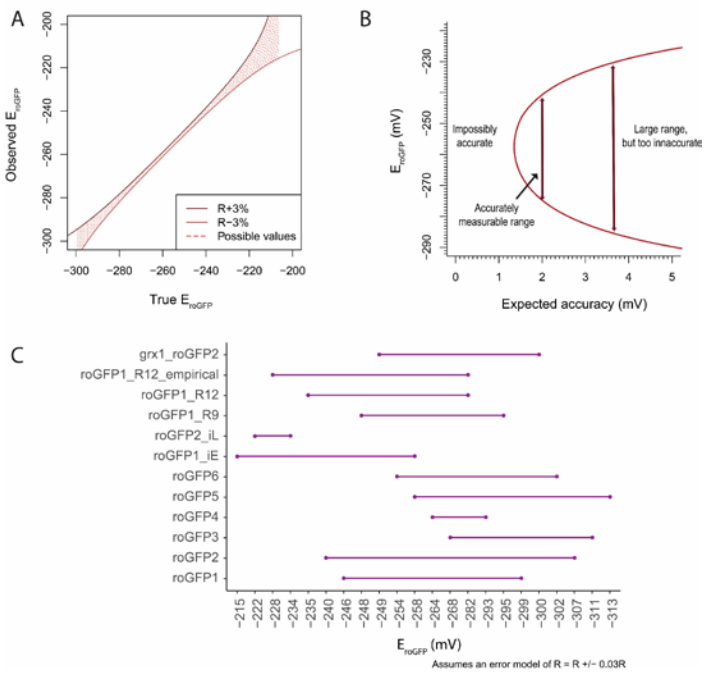

Figure 5. Errors **(A)** Map between expected E and observed E (B) Phase plot of roGFP1-R12 sensor (C) Relative suitability of many two-state redox sensors to detect changes to an accuracy of at least $2\ mV$, with 95% confidence.

1.3.4 Our framework applies to all ratiometric two-state biosensors

1.3.5 Interactive tools and documentation are publicly-available resources

1.4 References

1. Cannon MB, Remington SJ: Re-engineering redox-sensitive green fluorescent protein for improved response rate. *Protein Sci* 2006, 15(1):45-57.

2. Cannon MB, Remington SJ: Redox-sensitive green fluorescent protein: probes for dynamic intracellular redox responses. A review. *Methods Mol Biol* 2008, 476:51-65.

3. Hanson GT, Aggeler R, Oglesbee D, Cannon M, Capaldi RA, Tsien RY, Remington SJ: **Investigating mitochondrial redox potential with redox-sensitive green fluorescent protein indicators**. *J Biol Chem* 2004, **279**(13):13044-13053.

4. Romero-Aristizabal C, Marks DS, Fontana W, Apfeld J: Regulated spatial organization and sensitivity of cytosolic protein oxidation in Caenorhabditis elegans. *Nat Commun* 2014, 5:5020.

5. Meyer AJ, Dick TP: **Fluorescent protein-based redox probes**. *Antioxid Redox Signal* 2010, **13**(5):621-650.

2 Long-form narrative

2.1 Understanding the properties of roGFP1_R12

In the Apfeld lab, we use the redox-sensitive roGFP1_R12 biosensor to measure cellular patterns of glutathione redox potentials. We are not aware of any published work that comprehensively reviews the biochemical and biophysical properties of the sensor that allow us to infer glutathione redox potentials from fluorescence measurements. To better understand the conditions that the roGFP1_R12 is well-suited to measure, we (1) explicitly define the biochemical and biophysical properties of roGFP1_R12 and their maps to redox measurements, (2) present an analysis of the sensitivity of the sensor to our empirical microscopy imprecision, and (3) generalize our sensitivity analysis to any error model.

2.1.1 Defining a sensor

Any fluorescent sensor has a characteristic excitation-emission pattern. A two-state fluorescent sensor may have two excitation-emission patterns, one for each state. In the case of GFP-based two-state fluorescent sensors, we generally record emission around $508\ nm$. We can then describe the emission intensity (at $\sim 508\ nm$) as a function of excitation wavelength (Figure 1).

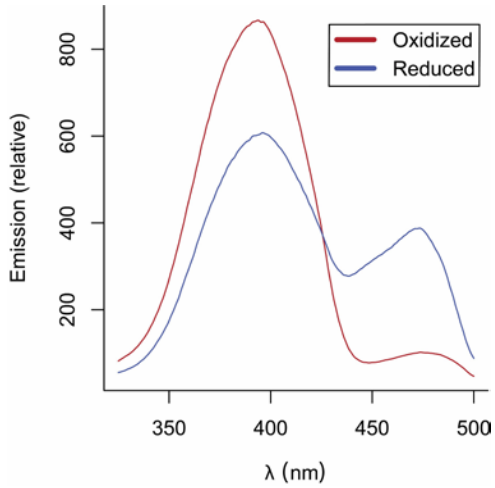

Figure 1. The emission intensity spectra for the roGFP1_R12 sensor in its oxidized and reduced states.

While an individual sensor will be either oxidized or reduced, a collection of sensors will be some fraction oxidized or reduced. In this case, the sum of the entire population of sensor emission will be the weighted average of all the oxidized and reduced sensors (Figure 2).

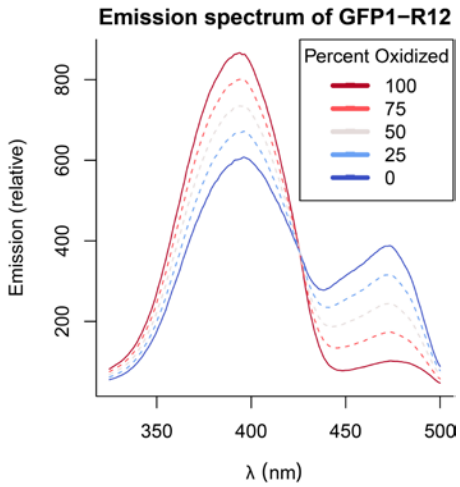

Figure 2. The emission intensity spectra for a population of roGFP1_R12 sensors.

We can use measurements of the emission intensity spectra to back-calculate the fraction of oxidized and reduced sensors, which informs us about the glutathione redox state of a cell. While it is generally not feasible to measure the entire spectra of a population of sensors, it is easier to record fluorescent measurements at single excitation wavelengths. Since single wavelength measurements are concentration-dependent, we measure at two wavelengths and record a ratiometric emission. With some sensors, ratiometric measurements dilute the signal, rendering it difficult to distinguish between different levels of oxidization. When sensors have a clear isosbestic point, like roGFP1_R12 has around $430\ nm$, ratiometric measurements amplify the signal, since oxidized sensors emit more fluorescence in one wavelength, but less in the other (Figure 3).

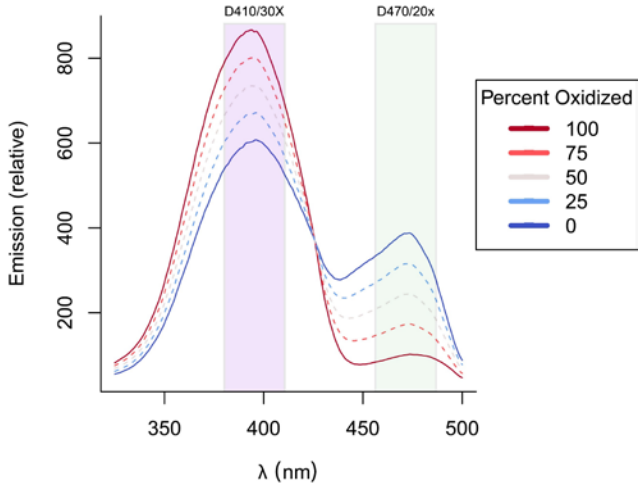

Figure 3. The emission intensity spectra for a population of roGFP1_R12 sensors with the band wavelengths of (purple) the D410/30X microscope filter and (green) the D470/20x microscope filter. These two filters will be automatically switched when a ratio measurement is taking, producing a $\frac{410\ nm}{470\ nm}$ ratio image.

2.1.2 Spectra-defined parameters define the map between ratio and redox

When we measure our sensor at a ratio of $R = \frac{410}{470}$, we can map between ratio and the fraction of oxidized sensors with:

$$OxD = \frac{R - R_{min}}{\mathrm{R} - R_{min} + \delta_{470}(R_{max} - \mathrm{R})}$$

And between ratio and the glutathione redox potential with:

$$E_{GSH} = E^{\circ}_{roGFP} - \frac{R_{gas}T}{2F}\ln\left(\delta_{470} * \frac{R_{max} - R}{R - R_{min}}\right)$$

Where R_{gas} is the universal gas constant, T is the temperature in Kelvin, F is the faraday constant, and E°_{roGFP} is the empirically-determined midpoint potential of the sensor. Full derivations can be found in Supplementary Note 1.

Three constants define the maps between R and OxD and E_{GSH}: the maximum possible ratio value, R_{max}, the minimum possible ratio value, R_{min}, and the relative allocation of the dynamic range in the second wavelength, δ_{470}. Each of these parameters can be calculated from the physical spectra of the sensor, if it is known. R_{min} can be calculated as the $\frac{410}{470}$ intensity ratio in the reduced state, R_{max} as the $\frac{410}{470}$ intensity ratio in the oxidized state, and δ_{470} as the ratio between oxidized and reduced in at $470\ nm$, $\frac{I_{470,Oxidized}}{I_{470,Reduced}}$ (Figure 4).

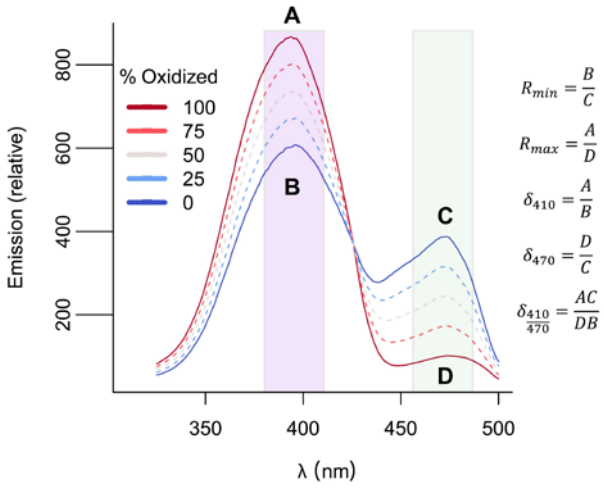

Figure 3. The emission intensity spectra for a population of roGFP1_R12 sensors with the band wavelengths of (purple) the D410/30X microscope filter and (green). **A**, **B**, **C**, and **D** are

labeled at $I_{410,Oxidized}$, $I_{410,Reduced}$, $I_{470,Oxidized}$, and $I_{470,Reduced}$, respectively. R_{min} and R_{max} are calculated as the $\frac{I_{410}}{I_{470}}$ ratios in the reduced and oxidized states, respectively. The δ_λ for any λ can be calculated as $\frac{I_{\lambda,Oxidized}}{I_{\lambda,Reduced}}$, and shown are the calculations for δ_{410}, δ_{470}, and $\delta_{\frac{410}{470}}$ as examples.

Given the R_{min}, R_{max}, and δ_λ values of a sensor, we can construct maps between ratio emission and the fraction oxidized (OxD) and the glutathione redox potential (E_{GSH}). Different values of R_{min} and R_{max} change the upper and lower bounds, but not the shape, of the transformation. The δ_λ value has different effects on the E_{GSH} and OxD maps.

The δ_λ value affects the linearity of the OxD map. Larger and smaller $\log(\delta_\lambda)$ values produce a more concave up or concave down map, respectively. A δ_λ value of 1 produces a linear map between R and OxD (Figure 4A).

The δ_λ value shifts the center of the E_{GSH} map. We can define the center of the map (the value at which the map between R and E is centered) as the adjusted midpoint potential E°_{adj}, where:

$$E(R) = E^\circ_{adj} - \frac{R_{gas}T}{2F}\ln\left(\frac{R_{max}-R}{R-R_{min}}\right) \; and$$

$$E^\circ_{adj} = E^\circ + \frac{RT}{2F} ln(\delta_{\lambda_2})$$

Larger and smaller $\log(\delta_\lambda)$ values shift the E_{GSH} map down and up, respectively. A map with a δ_λ value of 1 is centered at the midpoint potential (Figure 4B).

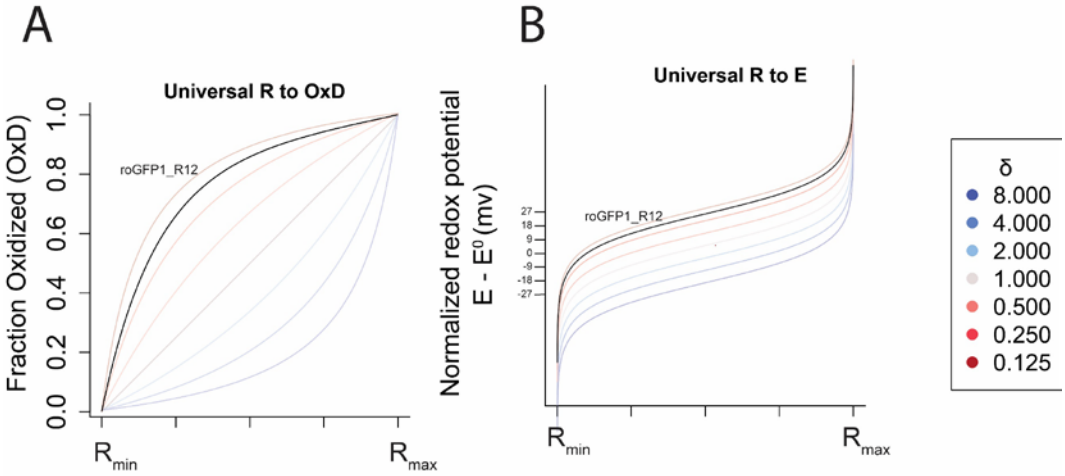

Figure 4. TODO: Add some more extreme deltas (16? 32?) (A) The map between ratio and fraction oxidized (OxD) always goes from R_{min} to R_{max} and the δ values determines the degree of linearity. roGFP1_R12 is concave down, since it has a δ_{470} of around 0.171. **(B)** The map between ratio and glutathione redox potential (E) always goes from R_{min} to R_{max} and the δ values determines the deviation of the apparent midpoint of the map from the true midpoint

potential. roGFP1_R12 has an apparent midpoint potential that is approximately $22\ mV$ higher than the true midpoint potential, since it has a δ_{470} of around 0.171.

2.1.3 Ratio-redox maps are affected by the choice of ratio wavelengths

The parameters that define the maps between R and OxD and E_{GSH} are defined by the sensor's spectra (Figure 3). It therefore follows that, by changing the wavelengths at which you measure a sensor's ratio intensity, you can also change the maps.

To demonstrate the wavelength-dependences of the OxD and E_{GSH} maps, we examined how a difference choice of the second wavelength (λ_2 in $R = \frac{I_{\lambda_1}}{I_{\lambda_2}}$) in the ratio measurement would affect the maps. The value of δ_{λ_2} in the published spectrum of roGFP1_R12 varies widely, from around 1.5 at $390\ nm$ to around 0.2 at $450\ nm$. Choosing values across the spectrum, the max between R and OxD ranged from concave up to concave down, and the map between R and E_{GSH} had midpoints ranging from $-270\ mV$ to $-244\ mV$ (Figure 5).

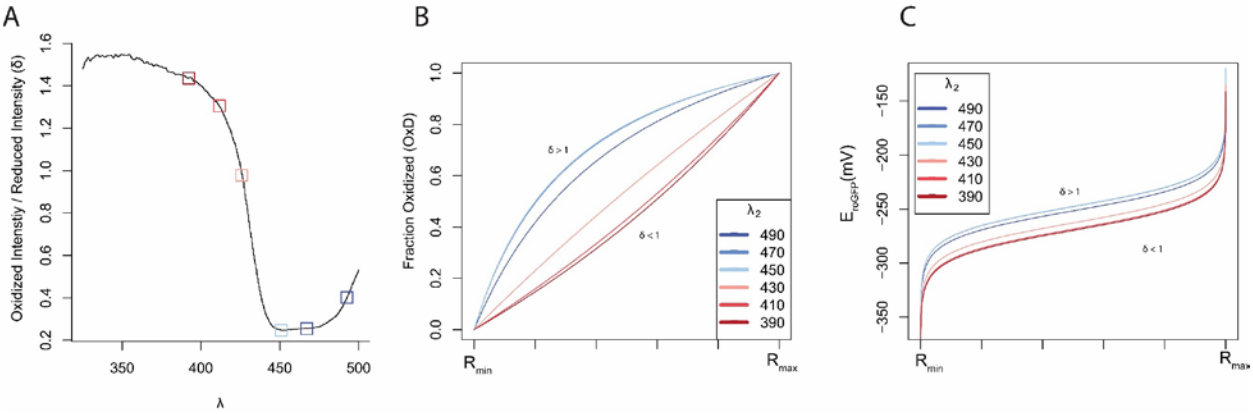

Figure 5. The choice of the second wavelength in the ratio image (λ_2) changes the map between ratio and biochemically-meaningful values in roGFP1_R12. **(A)** The value of δ_λ changes with the choice of second wavelength **(B)** The linearity of the map between R and OxD changes based on the choice of second wavelength. **(C)** The map between R and E_{GSH} is linearly scaled based on the choice of second wavelength.

2.2 Sensitivity analysis of the roGFP1_R12 sensor

Small, stochastic errors in measuring the can lead to much larger errors in measures of the fraction of oxidized sensors and the redox potential, especially near the maximum and minimum ratio values of the sensor (Supplementary Figure 1). The relative sensitivity of these values to changes in ratio can be described by their partial derivates (Supplementary Figure 2). Therefore, we can define a unique mapping between observed and 'true' redox potential values for any sensor (Figure 3A). This mapping allows us to create a phase plot of redox

potential values in which, for a given model of error in the ratio R, we can define a range of redox values well-suited to being measured to a given accuracy (Figure 3B). Using a set error model for R and a desired accuracy, we can compare the ranges of redox potentials that different sensors are well-suited to measure (Figure 3C).

2.2.1 Empirical observations

We sought to examine how imprecise microscopy measurements affect the estimates of the values of OxD and E_{GSSH}. First, we determined the imprecision in our microscopy setup. We found that the 95% confidence interval in our measurements was no larger than $(R_{True} * 0.97, R_{True} * 1.03)$, or a 3% relative error model described by $R_{Observed} = R_{True}(1 \pm 0.03)$ (Figure 6A, Supplementary Note 2).

When a 3% error in R, the error in OxD can be described as:

$$\Delta OxD = \left| \frac{[R(1 \pm 0.03)] - R_{min}}{[R(1 \pm 0.03)] - R_{min} + \delta_{470}(R_{max} - [R(1 \pm 0.03)])} - \frac{R - R_{min}}{\mathrm{R} - R_{min} + \delta_{470}(R_{max} - \mathrm{R})} \right|$$

And the error in glutathione redox potential as:

$$\Delta E = \left[-\frac{R_{gas}T}{2F} \ln\left(\frac{R_{max} - [R(1 \pm 0.03)]}{[R(1 \pm 0.03)] - R_{min}} \right) \right] - \left[-\frac{R_{gas}T}{2F} \ln\left(\frac{R_{max} - R}{R - R_{min}} \right) \right]$$

The propagated error into OxD relatively small. The error in E_{GSH} is also small near the midpoint but explodes near the edges of the map (Figure 6B, 6C)

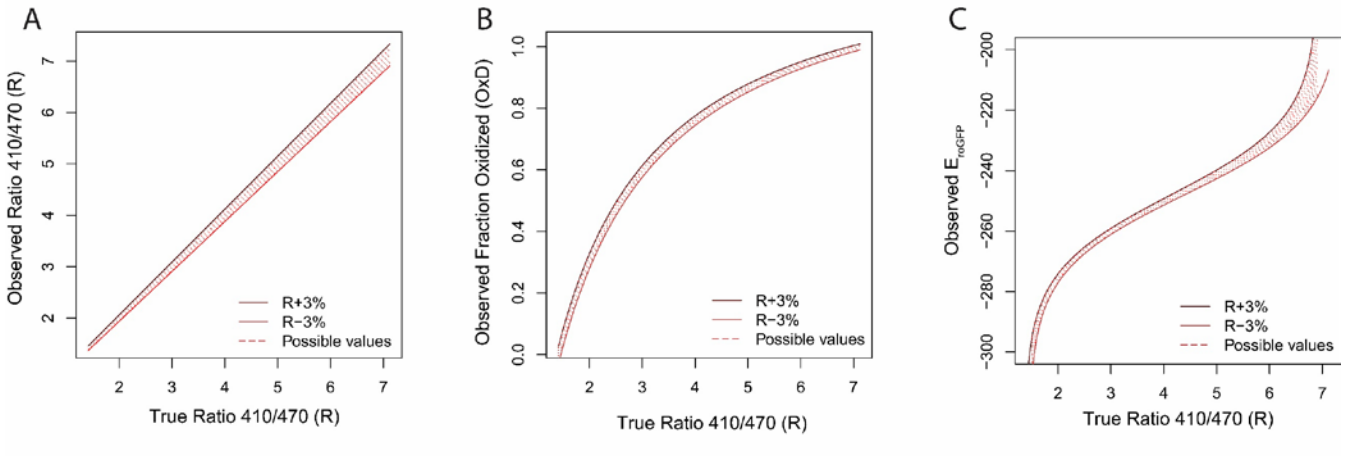

Figure 6. (A) Our empirically-observed error model of $R_{Observed} = R_{True} * (1 \pm 0.03)$. **(B)** The effect of 3% microscopy error on the estimate of fraction oxidized (OxD). **(C)** The effect of 3% microscopy error on the estimate of glutathione redox potential (E_{GSH}).

The relative sensitivity of the maps to a constant amount of error is given by the partial derivatives of those maps with respect to R. Note that the sensitivity of E_{GSH} is only dependent on the R_{min} and R_{max}, while the sensitivity of OxD also depends on δ_{λ_2} (Figure 7).

Figure 7. TODO: Combined sensitivities. (A) $\frac{\partial OxD}{R}$, with different values of delta shown (B) $\frac{\partial E}{R}$, which is always just bounded by the min and max.

We next sought to put our analysis into a more empirically-useful context. We noticed that all true ratio measurements map to some true glutathione redox potential. Using that observation, we modified the plot in Figure 6C to map between true redox potential values, and the ranges of values one may observe 95% of the time (Figure 9A). Then, we computed the maximum deviations from the true redox potential that one may observe at any given true redox potential (Figure 9B, 9C).

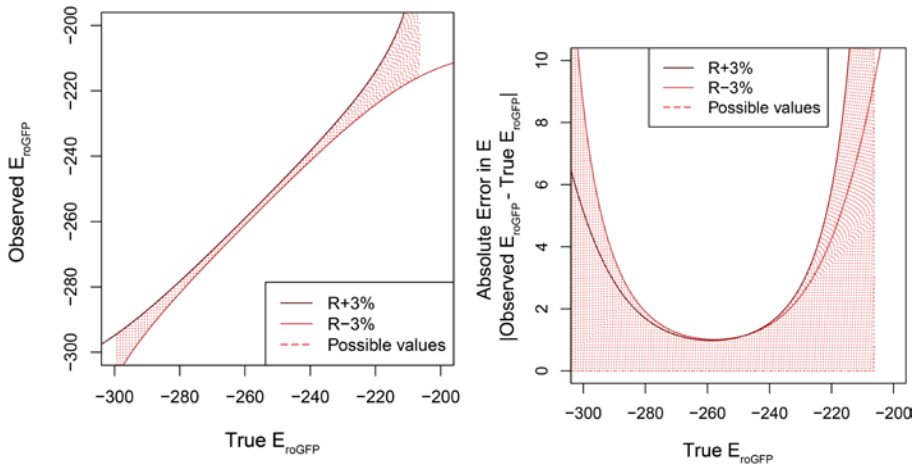

Figure 9. TODO: Combined errors. (A) True E vs Observed E, (B) True E vs raw error (C) True E vs absolute error

We observed that, at any true redox potential, there is some maximum amount of error that we could expect to see at that point, with 95% confidence (Figure 10A). By inverting the axes of that relationship, we can construct a phase plot. To use the phase plot, first pick the maximum

amount of inaccuracy you are willing to tolerate for an experiment. For example, we might want to measure redox potentials within $2\ mV$ of their actual values. Then, the cross sectional area of the phase curve represents the redox values that can be measured to that level of accuracy (Figure 10).

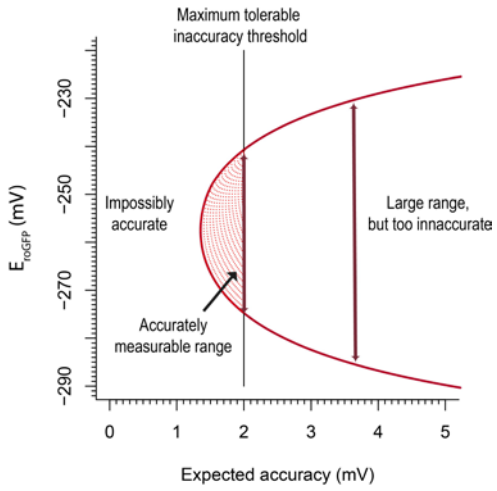

Figure 10. TODO: (A) Maximum amount of error at each redox potential (B) Phase plot

2.2.2 Theoretical framework

A phase plot can be made for any redox sensor, as long as we know (1) the physical characteristics of the sensor, specifically R_{min}, R_{max}, δ_{λ_2}, and $E°$, and (2) the precision of the microscope, specifically an error model in the form of a function $R_{Observed} = f(R_{expected})$ (Figure 11).

Figure 11. TODO: Phase plots at different error levels and different δ_{λ_2} values.

2.3 Applying of the framework to other redox sensors

Once we understood our framework, we sought to ask what ranges of glutathione redox potentials we could measure if we had used a different biosensor. Using publicly-available spectra data, we computed the ranges that 10 roGFP-based sensors would be suitable to measure to a precision of $2\ mV$ (Figure 12).

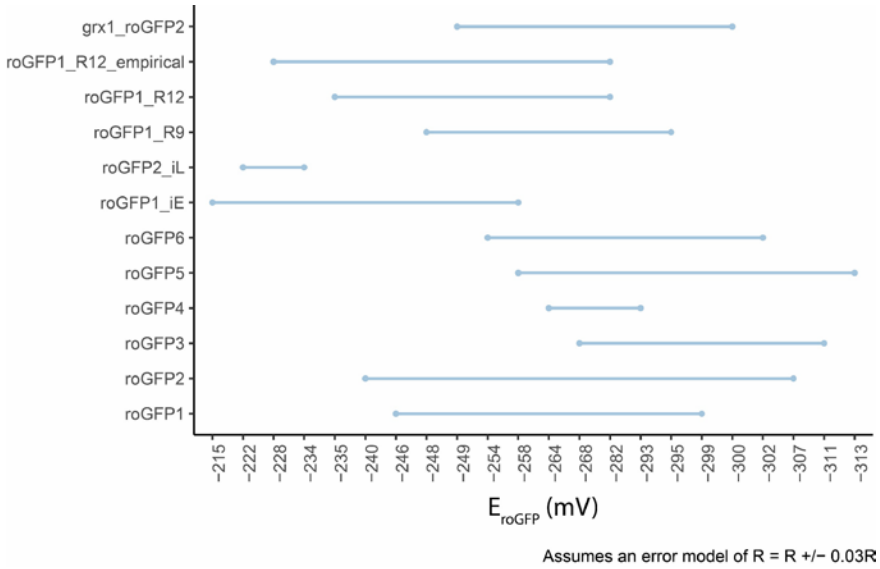

Figure 12. Ranges of redox potentials that publicly-available redox sensors are able to measure to an accuracy of $2\ mV$.

2.4 Generalizing the framework to any two-state, ratiometric sensor

2.5 Applying the more general framework to pH and ATP sensors

3 Supplementary material

3.1 Supplementary Note 1 — Derivations of ratio-redox maps

The intensity values emitted from the roGFP1-R12-containing tissue are recorded after being exposed to 410nm and 470nm light. The ratios between these emission values describe relative levels of tissue oxidation. For example, a 410/470 ratio of 2.0 indicates that a tissue is more oxidized than a ratio of 1.0. But how exactly does a ratio intensity value correspond to the proportion of oxidized tissues in a cell? Here we derive the equations for those maps.

3.1.1 Map from ratio intensity to degree of oxidation

Assume a fully reduced state. Then, the intensities observed at a wavelength λ are equal to the product of N_T, the total number of roGFP molecules, and $I_{\lambda,R}$, the intensity of each roGFP molecule at a given wavelength in the reduced state.

$$I_{\lambda,R} = N_T * I_{\lambda,R}$$

The same is true for the fully oxidized state:

$$I_{\lambda,X} = N_T * I_{\lambda,X}$$

At any redox state between maximally reduced and maximally oxidized, the intensity at a given wavelength is a weighted sum of the molecules found at either discretely oxidized or reduced state. We therefore can rewrite any observed intensity as the weighted sum of two states:

$$I_\lambda = \frac{N_X}{N_T} * I_{\lambda,X} + \frac{N_{Red}}{N_T} * I_{\lambda,R} \quad (1)$$

Because all sensor molecules must be in either an oxidized or reduced state, $N_R = N_T - N_X$. So, we can rewrite equation (1) as a function of only the fraction in one state:

$$I_\lambda = \frac{N_X}{N_T} * I_{\lambda,X} + (1 - \frac{N_X}{N_T}) * I_{\lambda,R} \quad (2)$$

Using equation (2), consider the intensity ratio taken after excitation at $\frac{\lambda_1}{\lambda_2}$:

$$\frac{I_{\lambda_1}}{I_{\lambda_2}} = \frac{\frac{N_X}{N_T} * I_{\lambda_1,X} + (1 - \frac{N_X}{N_T}) * I_{\lambda_1,R}}{\frac{N_X}{N_T} * I_{\lambda_2,X} + (1 - \frac{N_X}{N_T}) * I_{\lambda_2,R}}$$

For brevity, let $OxD = \frac{N_X}{N_T}$. Then cross-multiply:

$$I_{\lambda_1} * OxD * (I_{\lambda_2,X} + (1 - OxD) * I_{\lambda_2,R}) =$$

$$I_{\lambda_2} * OxD * (I_{\lambda_1,X} + (1 - OxD) * I_{\lambda_1 R})$$

Simplify and express OxD in terms of known quantities:

$$OxD = \frac{I_{\lambda_2} I_{\lambda_1,R} - I_{\lambda_1} I_{\lambda_2,R}}{I_{\lambda_1} I_{\lambda_2,X} - I_{\lambda_1} I_{\lambda_2,R} - I_{\lambda_2} I_{\lambda_1 X} + I_{\lambda_2} I_{\lambda_1,R}}$$

To further simplify, let:

$$R_{Red} = \frac{I_{\lambda_1,R}}{I_{\lambda_2,R}} = R_{min}$$

$$R_X = \frac{I_{\lambda_1,X}}{I_{\lambda_2,X}} = R_{max}$$

$$R = \frac{I_{\lambda_1}}{I_{\lambda_2}}$$

$$\delta_{\lambda 2} = \frac{I_{\lambda_{1,X}}}{I_{\lambda_{2_R}}}$$

We can now re-derive the definition of OxD in terms of ratio values.
First, re-arrange terms and multiply by $\frac{-1}{-1}$:

$$OxD = \frac{I_{\lambda_1} I_{\lambda_2,R} - I_{\lambda_2} I_{\lambda_1,R}}{I_{\lambda_1} I_{\lambda_2,R} - I_{\lambda_2} I_{,\lambda_1 R} + I_{\lambda_2} I_{\lambda_1 X} - I_{\lambda_2 X} I_{\lambda_1}}$$

Then factor out $I_{\lambda_2,R} I_{\lambda_2}$ from the numerator and denominator write some in terms of ratio values:

$$OxD = \frac{I_{\lambda_2,R} I_{\lambda_2} (\mathrm{R} - R_R)}{I_{\lambda_2,R} I_{\lambda_2} (\mathrm{R} - R_R + \delta_{\lambda 2}(R_X - \mathrm{R}))}$$

And simplify:

$$OxD = \frac{R - R_{min}}{\mathrm{R} - R_{min} + \delta_{\lambda 2}(R_{max} - \mathrm{R})} \quad (3)$$

Where $\delta_{\lambda 2}$ describes the simple intensity dynamic range after excitation at λ_2.

We can then describe the redox potential of the redox-sensitive sensor protein using the Nernst equation:

$$E_{roGFP} = E^{\circ}_{roGFP2} - \frac{RT}{2F} \ln\left(\frac{1 - OxD_{roGFP}}{OxD_{roGFP}}\right)$$

Where E°_{roGFP2} is the sensor's midpoint potential, R is the gas constant, T is the temperature in Kelvin, and F is the faraday constant.

If the sensor is in equilibrium with glutathione, the same equation also determines the redox potential of the glutathione couple:

$$E_{GSH} = E^{\circ}_{roGFP2} - \frac{RT}{2F} \ln\left(\frac{1 - OxD_{roGFP}}{OxD_{roGFP}}\right) \quad (4)$$

By plugging in the OxD equation (3), we can also express the glutathione redox potential as a function of R:

$$E_{GSH} = E^{\circ}_{roGFP2} - \frac{RT}{2F} \ln\left(\delta_{\lambda_2} \frac{R_{max} - R}{R - R_{min}}\right) \quad (4)$$

3.2 Supplementary Note 2 — Estimating empirical errors